Supplement of Biogeosciences, 20, 2499–2523, 2023
https://doi.org/10.5194/bg-20-2499-2023-supplement


Biogeosciences Open Access EGU

*Supplement of*

# All about nitrite: exploring nitrite sources and sinks in the eastern tropical North Pacific oxygen minimum zone

**John C. Tracey et al.**

*Correspondence to:* John C. Tracey (jt16@princeton.edu)

*Correspondence to:* John C. Tracey (jt16@alumni.princeton.edu)

**Supplementary Material:**

**Additional Information on Anammox and Denitrification Profiles (SR1805 and FK180624)**

In order to calculate the denitrification and anammox rates using Eq. (7 – 9) , the amount of 29 and 30 $N_2$ in nmol for each vial must first be calculated using the equations below:

$$29_{N_{2_{nmol}}} = (Slope_{STD\ Curve}) * \frac{29}{28_{A_M}} * \widehat{28}_{N_{2_{Peak\ Area}}} \quad \text{(S1)}$$

$$30_{N_{2_{nmol}}} = (Slope_{STD\ Curve}) * \frac{30}{28_{A_M}} * \widehat{28}_{N_{2_{Peak\ Area}}} \quad \text{(S2)}$$

Where:

$\frac{30}{28_{A_M}}$ *or* $\frac{29}{28_{A_M}}$ is the measured ratio in peak area units of the specific sample,

$\widehat{28}_{N_{2_{Peak\ Area}}}$ is the average 28 peak area across the time course (without outliers), and

$Slope_{STD\ Curve}$ is the standard curve slope in nmol / peak area units.

Outliers were defined as values more than three standard deviations away from the raw time course mean. Outlier points were not used to calculate the average 28 $N_2$ peak used in Eqs. (S1-2). The average 28 peak area across the time course was used as a data smoothing technique to remove variation due to small differences in the water volume aliquoted into each exetainer or to small amounts of $N_2$ that escaped purging.

After removing outlying 28 $N_2$ points, drift corrections, if necessary, were performed as follows. First, the 29 / 28 and 30 / 28 ratios of the standards from each mass spectrometer (MS) run were regressed using both linear and logarithmic models against the total N of each sample. If the regressions returned slopes significantly different from zero via a Student's T test (p values <0.05), a drift correction was performed using the best regression (as determined by $R^2$ and the residual mean square error (RMSE) values). Corrections were performed by using the best significant regression to calculate a theoretical value for each total N point. After this the difference between an "endpoint" (the endpoint varied from run to run - the highest or lowest theoretical value for one of the standards was used) and each theoretical value was calculated for every point. This difference was then added to the raw sample and standard values to correct for drift. After performing total N drift corrections, corrected ratios were re-plotted against total N to examine if the correction was successful. After performing a total N correction, samples were examined for drift due to the time in the mass spectrometer run. This was performed in an analogous manner to the total N drift correction.

Drift corrected 29 and 30 $N_2$ produced values were then checked for outliers across each time course. As above, points more than three standard deviations away from the time course

mean were discarded. After this, the drift corrected, outlier screened 29 and 30 $N_2$ produced values were used to calculate rates via Eq. (7 – 9). Importantly, the rates reported here were not all calculated using regressions from $t_0 - t_4$. Instead, regressions from $t_0 - t_2$, $t_0 - t_3$, and $t_0 - t_4$ were compared and the best regression was selected based on a combination of the $R^2$ and RMSE value. Rates due to a bottle effect (i.e., exponential growth of an N cycling microbe at the end of the incubation because incubation conditions changed over the course of the experiment to favor exponential growth) were removed by comparing linear and exponential models for any suspected time courses. If the exponential model was a better fit, the rate from that time course was not reported and the next shorter significant time course ($t_0 - t_2$, or $t_0 - t_3$) for that incubation was used.

For the SR1805 cruise, anammox rates calculated from the $^{15}NH_4^+$ and $^{15}NO_2^-$ tracers were similar in magnitude (Supplementary Table S3). As a result, the SR1805 anammox rates reported in Figs. 2, 3, 6, 7, 8, and 9 represent either the average of the rates calculated from the $^{15}NH_4^+$ and $^{15}NO_2^-$ tracers (if significant rates were returned for both tracers) or the rate from the tracer that returned a significant or positive rate with error bars above zero. The FK180624 anammox rates reported in Fig. S1 are from the $^{15}NO_2^-$ tracer alone.

## Additional Information for $NO_2^-$ Oxidation Rate Measurements

### Methods Details for Depth Profiles

The denitrifying bacterium culture seed (*Pseudomonas chloroaphis*) was prepared aerobically and frozen until needed. The denitrifiers were allowed to grow to high biomass for approximately five days so all $NO_3^-$ in the growth medium was consumed. The denitrifiers were then concentrated through centrifugation and resuspended in a medium that lacked $NO_3^-$. The

concentrate was distributed in 20 mL Grace vials (Manufacturer: Thermo Fisher Scientific, Bremen, Germany), sealed, and purged of $O_2$ with He for 3 – 5 hours. Grace vials were chosen because their straight shape allows for minimum $O_2$ contamination while purging. After removing $N_2$, exetainers were prepared for the denitrifier method by subsampling 1 mL and then adding 30 μL sulfamic acid to consume any residual ambient or tracer $NO_2^-$ present. After this, 30 μL of 5 N NaOH was added to return each sample to its original pH (Granger, J., & Sigman, 2009). The Grace vials were then injected with 1 mL of the sulfamic acid treated seawater samples and incubated overnight in the dark to convert $NO_3^-$ to $N_2O$. Five to six drops of 10 N NaOH was added to terminate the reactions in the vials, and 5-6 drops of Antifoam B were added so the solution would not foam when purged with helium by the mass spectrometer. Drift corrections, mechanism for selecting the best time course from $t_0 - t_2$, $t_0 - t_3$, and $t_0 - t_4$, and checks for bottle effects were conducted in similar ways to those described above for anammox and denitrification depth profiles.

**Method Details for Dismutation Experiments**

Measurements of anammox, denitrification, and $NO_2^-$ oxidation for the dismutation tests were conducted as above except for the following changes:

(1) For the $^{15}NO_3^-$ measurements of the dismutation experiments, 200 μL of acidified seawater sample was injected into each Grace vial instead of the 1 mL used in the depth profiles.

(2) For the anammox and denitrification measurements of the dismutation experiments, unlike in the depth profile experiments, each replicate within the 5 points of our 15 member time course was run on separate MS runs (i.e. $t_{0\ point\ 1}$, $t_{1\ point\ 1}$, $t_{2\ point\ 1}$, $t_{3\ point\ 1}$, and $t_{4\ point\ 1}$, were run together while $t_{0\ point\ 2}$, $t_{1\ point\ 2}$, $t_{2\ point\ 2}$, $t_{3\ point\ 2}$, and $t_{4\ point\ 2}$ and $t_{0\ point\ 3}$, $t_{1\ point\ 3}$, $t_{2\ point\ 3}$, $t_{3\ point\ 3}$, and $t_{4\ point\ 3}$

were run on separate runs. Samples were corrected for time and linearity in each separate MS run as in the depth profile experiments. After performing these corrections, the fifteen points from each time course were combined; however, the resulting time courses often had widely disparate ranges. In order to reduce the error of the rate regression, the range between mini time courses (i.e., $t_{0\ point\ 1}$, $t_{1\ point\ 1}$, $t_{2\ point\ 1}$, $t_{3\ point\ 1}$, and $t_{4\ point\ 1}$ is one "mini" course out of three per depth), was condensed using the following method:

(a) Linear regressions for each of the mini time courses were calculated.

(b) Using these regressions, theoretical values at each point in the mini time courses were calculated.

(c) The average of these theoretical values for each of the three mini time courses was calculated.

(d) A linear regression for the whole time course was calculated.

(e) Using the whole time course regression, theoretical values at each of the five time points in the full length time course was calculated.

(f) The average of these five theoretical values was calculated.

(g) The difference between each mini time course's average and the full length average was calculated.

(h) This difference was added to each point in the run to condense the mini time courses' range.

The remaining calculations were performed as in the depth profile experiments.

| Station | OMZ region | Bottom Z (m) | Coordinates | Depths (m) | Feature |
|---|---|---|---|---|---|
| PS1 | Offshore | 4100 | 10N | 30 | Oxic surface |
| | | | 113W | 60 | Oxycline |
| | | | | 70 | Oxycline |
| | | | | 90 | ODZ top |
| | | | | 100 | ODZ top |
| | | | | 110 | ODZ top |
| | | | | 150 | ODZ top |
| | | | | 260 | ODZ core |
| | | | | 500 | ODZ core |
| | | | | 1000 | Oxycline |
| PS2 | Open ocean | 3000 | 15.76N | 60 | Oxic surface |
| | | | 105W | 75 | Oxycline |
| | | | | 95 | ODZ top |
| | | | | 120 | ODZ top |
| | | | | 150 | ODZ top |
| | | | | 200 | ODZ top/SNM |
| | | | | 250 | ODZ core/SNM |
| | | | | 300 | ODZ core |
| | | | | 500 | ODZ core |
| | | | | 850 | ODZ core |
| PS3 | Coastal | 1030 | 17.68N | 16 | Oxycline |
| | | | 102.35W | 25 | Oxycline |
| | | | | 35 | Oxycline |
| | | | | 45 | ODZ top |
| | | | | 60 | ODZ top |
| | | | | 70 | ODZ top |
| | | | | 100 | ODZ top |
| | | | | 160 | ODZ top/SNM |
| | | | | 250 | ODZ core |
| | | | | 800 | ODZ core |

**Supplementary Table S1:** Sampling depths and geography for $NH_4^+$ oxidation, $NO_3^-$ reduction, $NO_2^-$ oxidation, anammox, and denitrification profiles (SR1805). Features are classified based on their potential density and $O_2$ concentrations. ODZ core samples have a $\sigma_\theta > 26.4$ (Babbin et al., 2020). ODZ top, oxycline, and oxic surface samples have a $\sigma_\theta < 26.4$ (Babbin et al., 2020).

| Station | OMZ region | Bottom Z (m) | Coordinates | Depths (m) | Feature |
|---|---|---|---|---|---|
| 2 | Open ocean | 3450 | 14N, 103W | 102 | Oxycline |
| | | | | 105 | ODZ top |
| | | | | 120 | ODZ top |
| | | | | 130 | ODZ top |
| | | | | 200 | ODZ top/SNM |
| | | | | 395 | ODZ core |
| 3 | Open ocean | 3000 | 14N, 104W | 120 | ODZ top |
| | | | | 140 | ODZ top |
| | | | | 170 | ODZ top |
| | | | | 250 | ODZ core |
| 9 | Open ocean | 3250 | 14N, 110W | 96 | Oxycline |
| | | | | 100 | Oxycline |
| | | | | 105 | ODZ top |
| | | | | 115 | ODZ top |
| | | | | 130 | ODZ top |
| | | | | 160 | ODZ top/SNM |
| | | | | 168 | ODZ core/SNM |
| | | | | 175 | ODZ core/SNM |
| | | | | 200 | ODZ core/SNM |
| | | | | 250 | ODZ core/SNM |
| | | | | 300 | ODZ core |
| | | | | 375 | ODZ core |
| | | | | 475 | ODZ core |
| | | | | 730 | ODZ core |
| 11 | Open ocean | 4000 | 14N, 112W | 116 | ODZ top |
| | | | | 320 | ODZ core |
| 12 | Open ocean | 4100 | 14N, 113W | 103 | ODZ top |
| | | | | 120 | ODZ top |
| | | | | 150 | ODZ top/SNM |
| | | | | 610 | ODZ core |
| 14 | Open ocean | 4100 | 14N, 115W | 125 | ODZ top/SNM |
| | | | | 323 | ODZ core |
| 15 | Open ocean | 4200 | 14N, 116W | 135 | ODZ top |
| | | | | 160 | ODZ top |
| 18 | OMZ boundary | 4100 | 17N, 119W | 130 | Oxycline |
| | | | | 160 | Oxycline |
| | | | | 200 | ODZ core |

**Supplementary Table S2:** Sampling depths and geography for anammox, and denitrification profiles (FK180624). Features are classified based on their potential density and $O_2$ concentrations. ODZ core samples have a $\sigma_\theta > 26.4$ (Babbin et al., 2020). ODZ top, oxycline, and oxic surface samples have a $\sigma_\theta < 26.4$ (Babbin et al., 2020).

| **Depth (m)** | **Denitrification** | | **Anammox ($^{15}NH_4^+$)** | | **Anammox ($^{15}NO_2^-$)** | | **Consensus anammox** | |
|---|---|---|---|---|---|---|---|---|
| | Rate | Error | Rate | Error | Rate | Error | Rate | Error |
| PS1 | | | | | | | | |
| 30 | 0 | 0 | 0 | 0 | 0 | 0 | 0 | 0 |
| 60 | 3.9 | 3.2 | 0 | 0 | 0 | 0 | 0 | 0 |
| 70 | 4.8 | 2.8 | 0 | 0 | 3.2 | 3.0 | 3.2 | 3.0 |
| 100 | 0 | 0 | 0.71 | 0.53 | **2.6** | **0.98** | **2.6** | **0.98** |
| 150 | 0 | 0 | 2.2 | 1.0 | **0.36** | **0.11** | **0.36** | **0.11** |
| 260 | 0 | 0 | **3.8** | **1.3** | **0.36** | **0.16** | **2.1** | **0.74** |
| 500 | **2.5** | **0.98** | 0 | 0 | 5.0 | 2.2 | 5.0 | 2.2 |
| 1000 | 0 | 0 | 0.74 | 0.7 | 0 | 0 | 0.74 | 0.7 |
| | | | | | | | | |
| PS2 | | | | | | | | |
| 120 | 0 | 0 | 1.2 | 0.86 | 0 | 0 | 1.2 | 0.86 |
| 150 | 0 | 0 | 0 | 0 | 2.9 | 2.3 | 2.9 | 2.3 |
| 200 | **7.2** | **2.5** | **1.6** | **0.46** | 0 | 0 | **1.6** | **0.46** |
| 250 | 3.3 | 2.0 | **4.3** | **1.1** | **4.1** | **1.2** | **4.2** | **1.2** |
| 300 | **1.6** | **0.58** | 0 | 0 | 0 | 0 | 0 | 0 |
| 500 | 0 | 0 | 0 | 0 | 0.19 | 0.11 | 0.19 | 0.11 |
| 850 | 0 | 0 | **4.5** | **1.4** | 0 | 0 | **4.5** | **1.4** |
| | | | | | | | | |
| PS3 | | | | | | | | |
| 16 | 0.8 | 0.53 | 0 | 0 | 0.52 | 0.41 | 0.52 | 0.41 |
| 25 | **1.2** | **0.33** | 0 | 0 | **1.0** | **0.35** | **1.0** | **0.35** |
| 35 | 0 | 0 | 0 | 0 | 0.53 | 0.27 | 0.53 | 0.27 |
| 45 | 0 | 0 | 0.24 | 0.21 | 0 | 0 | 0.24 | 0.21 |
| 60 | 0.33 | 0.28 | **1.2** | **0.32** | **0.89** | **0.29** | **1.1** | **0.31** |
| 70 | 0.7 | 0.33 | **0.83** | **0.29** | **1.0** | **0.18** | **0.93** | **0.23** |
| 100 | 0 | 0 | **1.7** | **0.31** | **1.3** | **0.4** | **1.5** | **0.35** |
| 160 | 1.9 | 0.89 | **0.69** | **0.21** | **2.4** | **0.8** | **1.5** | **0.5** |
| 250 | 0 | 0 | **1.2** | **0.35** | 0.94 | 0.71 | **1.2** | **0.35** |
| 800 | 0.47 | 0.33 | **0.58** | **0.16** | 0.34 | 0.26 | **0.58** | **0.16** |

**Supplementary Table S3:** Comparison of anammox rates calculated from $^{15}NH_4^+$ and $^{15}NO_2^-$ and denitrification rates from SR1805 cruise. Rates in bold are significantly different from zero. The consensus anammox rate was determined by (1) averaging the rates from the two tracers if both tracers returned a significant positive rate or (2) taking the rate from the tracer that returned a significant rate if the other tracer returned an insignificant rate or (3) taking the rate from the tracer that returned an insignificant but positive rate with error bars above zero if the other tracer returned a rate of zero.

| Cruise | Station | Target O2 (nM) | Depth (m) | Cast | Ambient O2 (µM) Unnormalized |
|---|---|---|---|---|---|
| SR1805 | PS1 | 1 | 93 | 4 | -0.87 |
| SR1805 | PS1 | 10 | 110 | 10 | -0.833 |
| SR1805 | PS1 | 100 | 110 | 14 | -0.257 |
| SR1805 | PS1 | 1000 | 110 | 18 | -0.549 |
| SR1805 | PS1 | 10000 | 100 | 23 | -0.026 |
| SR1805 | PS2 | 1 | 100 | 31 | -0.76 |
| SR1805 | PS2 | 10 | 113 | 37 | -0.096 |
| SR1805 | PS2 | 100 | 130 | 42 | -0.878 |
| SR1805 | PS2 | 1000 | 120 | 47 | -0.016 |
| SR1805 | PS2 | 10000 | 110 | 50 | -0.777 |
| SR1805 | PS3 | 1 | 60 | 70 | 0.274 |
| SR1805 | PS3 | 10 | 45 | 76 | 0.042 |
| SR1805 | PS3 | 100 | 50 | 81 | -0.806 |
| SR1805 | PS3 | 1000 | 46 | 85 | -0.795 |
| SR1805 | PS3 | 10000 | 60 | 88 | -0.859 |
| FK180624 | 2 | 10 | 120 | 2 | 1.329 |
| FK180624 | 2 | 1000 | 120 | 2 | 1.329 |
| FK180624 | 2 | 100 | 120 | 4 | 1.174 |
| FK180624 | 2 | 3000 | 120 | 4 | 1.174 |
| FK180624 | 9 | 1000 | 110 | Aft 67 | 2.0 |
| FK180624 | 9 | 1000 | 105 | Frank 197 | 2.2 |
| FK180624 | 9 | 3000 | 120 | 9 | 1.09 |
| FK180624 | 15 | 100 | 110 | 1 | 1.633 |
| FK180624 | 18 | 10000 | 105 | 1 | 12.138 |
| FK180624 | 2 | 10 | 120 | 2 | 1.329 |
| FK180624 | 2 | 1000 | 120 | 2 | 1.329 |
| FK180624 | 2 | 100 | 120 | 4 | 1.174 |
| FK180624 | 2 | 3000 | 120 | 4 | 1.174 |
| FK180624 | 9 | 1000 | 110 | Aft 67 | 2.0 |
| FK180624 | 9 | 1000 | 105 | Frank 197 | 2.2 |
| FK180624 | 9 | 3000 | 120 | 9 | 1.09 |
| FK180624 | 15 | 100 | 110 | 1 | 1.633 |
| FK180624 | 18 | 10000 | 105 | 1 | 12.138 |

**Supplementary Table S4:** Ambient $O_2$ concentrations for the sample water used in the $NO_2^-$ oxidation $O_2$ manipulation experiments on the SR1805 and FK180624 cruises.

| Station | Depth (m) | $NH_4^+$ oxidation | Maximum N loss from $NH_4^+$ oxidation | Anammox | Denitrification | Total N loss | Percent N loss due to $NH_4^+$ oxidation | $O_2$ |
|---|---|---|---|---|---|---|---|---|
| PS1 | 30 | **0.0010** | 0.0005 | 0.00 | 0.00 | 0.00 | 100 | 199.2 |
| PS1 | 60 | **0.8392** | 0.4196 | 0.00 | 3.9 | 3.9 | 10.7 | 108.7 |
| PS1 | 70 | **1.0803** | 0.5402 | 3.2 | 4.8 | 8.0 | 6.7 | 21.9 |
| PS1 | 90 | **0.2605** | 0.1302 | 0.0 | 0.0 | 0.0 | 100 | 0.2 |
| PS1 | 100 | **0.3070** | 0.1535 | **2.6** | 0.0 | 2.6 | 5.9 | 0.5 |
| PS1 | 110 | **0.0280** | 0.0140 | 0.00 | 0.00 | 0.00 | 100 | -0.1 |
| PS1 | 150 | **0.0014** | 0.0007 | **0.36** | 0.00 | 0.36 | 0.2 | 0.4 |
| PS1 | 260 | **0.0005** | 0.0003 | **2.1** | 0.0 | 2.1 | 0.0 | 2.9 |
| PS1 | 500 | **0.0002** | 0.0001 | 5.0 | **2.5** | 7.6 | 0.0 | -0.1 |
| PS1 | 1000 | **0.0002** | 0.0001 | 0.7 | 0.0 | 0.7 | 0.0 | 30.1 |
| PS2 | 60 | **0.0293** | 0.0146 | 0.0 | 0.0 | 0.0 | 100 | 174.5 |
| PS2 | 75 | **2.7476** | 1.3738 | 0.0 | 0.0 | 0.0 | 100 | 47.0 |
| PS2 | 95 | **0.9789** | 0.4894 | 0.0 | 0.0 | 0.0 | 100 | 3.2 |
| PS2 | 120 | **0.0093** | 0.0046 | 1.2 | 0.0 | 1.2 | 0.4 | -0.1 |
| PS2 | 150 | **0.0024** | 0.0012 | 2.9 | 0.0 | 2.9 | 0.0 | -0.1 |
| PS2 | 200 | **0.0025** | 0.0012 | **1.6** | **7.2** | 8.7 | 0.0 | 0.0 |
| PS2 | 250 | 0.0 | 0.0 | **4.2** | 3.3 | 7.5 | 0.0 | 1.2 |
| PS2 | 300 | **0.0** | 0.0 | 0.00 | **1.6** | 1.6 | 0.0 | -0.2 |
| PS2 | 500 | **0.0005** | 0.0003 | 0.19 | 0.00 | 0.19 | 0.1 | 0.1 |
| PS2 | 850 | 0.0 | 0.0 | **4.5** | 0.0 | 4.5 | 0.0 | 1.5 |
| PS3 | 16 | 0.0 | 0.0 | 0.52 | 0.80 | 1.3 | 0.0 | 90.2 |
| PS3 | 25 | **11.7272** | 5.8636 | **1.0** | **1.2** | 2.2 | 262 | 27.7 |
| PS3 | 35 | **6.3850** | 3.1925 | 0.53 | 0.00 | 0.53 | 601 | 1.9 |
| PS3 | 45 | 0.0 | 0.0 | 0.24 | 0.00 | 0.24 | 0.0 | -0.2 |

| Station | Depth (m) | $NH_4^+$ oxidation | Maximum N loss from $NH_4^+$ oxidation | Anammox | Denitrification | Total N loss | Percent N loss due to $NH_4^+$ oxidation | $O_2$ |
|---|---|---|---|---|---|---|---|---|
| PS3 | 60 | **0.1832** | 0.0916 | **1.1** | 0.33 | 1.4 | 6.6 | -0.3 |
| PS3 | 70 | 0.00 | 0.0 | **0.93** | 0.70 | 1.6 | 0.0 | 0.0 |
| PS3 | 100 | **0.0294** | 0.0147 | **1.5** | 0.0 | 1.5 | 1.0 | 0.1 |
| PS3 | 160 | **0.0061** | 0.0031 | **1.5** | 1.9 | 3.4 | 0.1 | 0.0 |
| PS3 | 250 | 0.0000 | 0.0000 | **1.2** | 0.0 | 1.2 | 0.0 | 0.0 |
| PS3 | 800 | **0.0345** | 0.0173 | **0.58** | 0.47 | 1.1 | 1.6 | 0.3 |

**Supplementary Table S5:** N loss due to $NH_4^+$ oxidation does not contribute a large fraction (> 10% of total N loss) of the total N loss except in oxic depths or depths where denitrification and anammox are low (< 1 nM $N_2$ $d^{-1}$). $NH_4^+$ oxidation rates and the maximum N loss from $NH_4^+$ oxidation rates are in shown in nmol N $d^{-1}$ and nmol $N_2$ $d^{-1,}$ respectively. Maximum N loss from $NH_4^+$ oxidation rates were calculated by unrealistically assuming that all $^{15}N\text{-}NO_2^-$ produced in $NH_4^+$ oxidation was converted to $N_2$. Anammox, denitrification, and total N loss are shown in nmol $N_2$ $d^{-1}$ and $O_2$ is shown in µM. Raw $NH_4^+$ oxidation, anammox, and denitrification rates that are significantly different from zero are shown in bold.

| Regression | Slope | Error | $R^2$ | P value | Line type | Color |
|---|---|---|---|---|---|---|
| Shallow boundary – all data | 0.56 | 0.059 | 0.55 | 1.4e-14 | Solid | Orange |
| ODZ core – all data | 0.45 | 0.053 | 0.54 | 9.5e-12 | Solid | Teal |
| Shallow boundary – 2018 only | 0.29 | 0.10 | 0.16 | 0.009 | Dashed | Orange |
| ODZ core – 2018 only | 0.35 | 0.038 | 0.79 | 2.5e-9 | Dashed | Teal |
| Shallow boundary – 2012-13 only | 0.64 | 0.073 | 0.69 | 3.1e-10 | Dotted | Orange |
| ODZ core – 2012-13 only | 1.1 | 0.13 | 0.68 | 2.3e-10 | Dotted | Teal |

**Supplementary Table S6:** Regression statistics for Fig. 9A (plot of denitrification vs. anammox rates).

| Station | Depth (m) | AMX Rate (nM $N_2$ $d^{-1}$) | DN Rate (nM $N_2$ $d^{-1}$) | $NO_2^-$ (µM) | $NH_4^+$ (nM) | Added $^{15}NO_2^-$ (µM) | Added $^{15}NH_4^+$ (nM) | $NH_4^+$ Enrichment | $NO_2^-$ Enrichment |
|---|---|---|---|---|---|---|---|---|---|
| PS1 | 30 | 0.00 | 0.00 | 0.02 | 3.15 | 3 | 3000 | 953.1 | 188.5 |
| PS1 | 60 | 0.00 | 0.00 | 1.37 | 31.36 | 3 | 3000 | 96.7 | 3.2 |
| PS1 | 70 | 0.00 | 0.00 | 0.30 | 4.46 | 3 | 3000 | 673.0 | 11.1 |
| PS1 | 90 | 0.00 | 0.00 | 0.01 | 45.93 | 3 | 3000 | 66.3 | 380.7 |
| PS1 | 100 | 2.61 | 0.00 | 0.01 | 32.99 | 3 | 3000 | 91.9 | 268.9 |
| PS1 | 110 | 0.00 | 0.00 | 0.02 | 2.98 | 3 | 3000 | 1008.9 | 188.5 |
| PS1 | 150 | 0.36 | 0.00 | 0.00 | 2.11 | 3 | 3000 | 1422.9 | 2001.0 |
| PS1 | 260 | 2.07 | 0.00 | 0.06 | 1.98 | 3 | 3000 | 1513.9 | 53.8 |
| PS1 | 500 | 0.00 | 2.53 | 0.01 | 3.78 | 3 | 3000 | 794.3 | 527.3 |
| PS1 | 1000 | 0.00 | 0.00 | 0.02 | 5.56 | 3 | 3000 | 540.2 | 159.7 |
| PS2 | 60 | 0.00 | 0.00 | 0.05 | 35.82 | 3 | 3000 | 84.7 | 63.6 |
| PS2 | 75 | 0.00 | 0.00 | 0.13 | 13.60 | 3 | 3000 | 221.5 | 24.8 |
| PS2 | 95 | 0.00 | 0.00 | 0.06 | 13.65 | 3 | 3000 | 220.8 | 51.1 |
| PS2 | 120 | 0.00 | 0.00 | 0.28 | 23.53 | 3 | 3000 | 128.5 | 11.7 |
| PS2 | 150 | 0.00 | 0.00 | 1.16 | 2.13 | 3 | 3000 | 1409.4 | 3.6 |
| PS2 | 200 | 1.56 | 7.15 | 1.82 | 1.81 | 3 | 3000 | 1657.7 | 2.6 |
| PS2 | 250 | 4.17 | 0.00 | 1.92 | 5.03 | 3 | 3000 | 597.0 | 2.6 |
| PS2 | 300 | 0.00 | 1.60 | 1.45 | 6.86 | 3 | 3000 | 438.6 | 3.1 |
| PS2 | 500 | 0.00 | 0.00 | 0.00 | 3.65 | 3 | 3000 | 823.4 | * |
| PS2 | 850 | 4.49 | 0.00 | 0.00 | 1.46 | 3 | 3000 | 2052.6 | * |
| PS3 | 16 | 0.00 | 0.00 | 0.08 | 302.03 | 3 | 3000 | 10.9 | 37.4 |
| PS3 | 25 | 1.05 | 1.19 | 0.58 | 250.57 | 3 | 3000 | 13.0 | 6.2 |
| PS3 | 35 | 0.00 | 0.00 | 0.27 | 9.49 | 3 | 3000 | 317.0 | 12.1 |
| PS3 | 45 | 0.00 | 0.00 | 0.23 | 8.85 | 3 | 3000 | 340.1 | 14.2 |
| PS3 | 60 | 1.06 | 0.00 | 0.25 | 1.37 | 3 | 3000 | 2196.9 | 13.0 |
| PS3 | 70 | 0.93 | 0.00 | 0.16 | 4.26 | 3 | 3000 | 704.8 | 19.4 |
| PS3 | 100 | 1.49 | 0.00 | 2.23 | 5.02 | 3 | 3000 | 598.2 | 2.3 |
| PS3 | 160 | 1.52 | 0.00 | 2.60 | 4.70 | 3 | 3000 | 638.8 | 2.2 |

| Station | Depth (m) | AMX Rate (nM $N_2$ $d^{-1}$) | DN Rate (nM $N_2$ $d^{-1}$) | $NO_2^-$ (µM) | $NH_4^+$ (nM) | Added $^{15}NO_2^-$ (µM) | Added $^{15}NH_4^+$ (nM) | $NH_4^+$ Enrichment | $NO_2^-$ Enrichment |
|---|---|---|---|---|---|---|---|---|---|
| PS3 | 250 | 1.15 | 0.00 | 1.96 | 5.73 | 3 | 3000 | 524.5 | 2.5 |
| PS3 | 800 | 0.58 | 0.00 | 0.00 | 6.35 | 3 | 3000 | 473.1 | * |
| 2 | 102 | 0.00 | 0.00 | 0.05 | N/A | 2 | N/A | N/A | 40.5 |
| 2 | 105 | 2.21 | 0.00 | 0.02 | N/A | 2 | N/A | N/A | 132.3 |
| 2 | 120 | 4.98 | 0.80 | 0.25 | N/A | 2 | N/A | N/A | 9.0 |
| 2 | 130 | 0.00 | 3.38 | 1.91 | N/A | 2 | N/A | N/A | 2.0 |
| 2 | 200 | 0.89 | 1.42 | 2.03 | N/A | 2 | N/A | N/A | 2.0 |
| 2 | 395 | 1.49 | 0.00 | 0.24 | N/A | 2 | N/A | N/A | 9.3 |
| 3 | 120 | 6.12 | 0.00 | 0.17 | N/A | 2 | N/A | N/A | 13.1 |
| 3 | 140 | 2.62 | 1.31 | 1.46 | N/A | 2 | N/A | N/A | 2.4 |
| 3 | 170 | 2.30 | 0.00 | 1.72 | N/A | 2 | N/A | N/A | 2.2 |
| 3 | 250 | 5.58 | 2.99 | 2.02 | N/A | 2 | N/A | N/A | 2.0 |
| 9 (7/6) | 105 | 2.23 | 0.00 | 0.03 | N/A | 2 | N/A | N/A | 76.9 |
| 9 (7/6) | 115 | 2.74 | 0.00 | 0.06 | N/A | 2 | N/A | N/A | 34.0 |
| 9 (7/6) | 130 | 4.75 | 0.00 | 1.41 | N/A | 2 | N/A | N/A | 2.4 |
| 9 (7/6) | 160 | 0.00 | 2.08 | 1.91 | N/A | 2 | N/A | N/A | 2.0 |
| 9 (7/6) | 168 | 3.67 | 0.00 | 1.52 | N/A | 2 | N/A | N/A | 2.3 |
| 9 (7/6) | 175 | 0.00 | 1.40 | 1.57 | N/A | 2 | N/A | N/A | 2.3 |
| 9 (7/6) | 250 | 2.82 | 0.00 | 1.81 | N/A | 2 | N/A | N/A | 2.1 |
| 9 (7/6) | 375 | 2.69 | 0.70 | 0.00 | N/A | 2 | N/A | N/A | * |
| 9 (7/9) | 96 | 1.53 | 1.52 | 0.03 | N/A | 2 | N/A | N/A | 69.3 |
| 9 (7/9) | 100 | 1.83 | 2.51 | 0.03 | N/A | 2 | N/A | N/A | 67.9 |
| 9 (7/9) | 200 | 19.98 | 7.03 | 1.28 | N/A | 2 | N/A | N/A | 2.6 |
| 9 (7/9) | 200 | 3.41 | 1.78 | 1.46 | N/A | 2 | N/A | N/A | 2.4 |
| 9 (7/9) | 300 | 1.34 | 0.00 | 0.99 | N/A | 2 | N/A | N/A | 3.0 |
| 9 (7/9) | 475 | 1.23 | 0.00 | 0.00 | N/A | 2 | N/A | N/A | * |
| 9 (7/9) | 730 | 2.42 | 0.67 | 0.00 | N/A | 2 | N/A | N/A | * |
| 11 | 116 | 1.92 | 0.00 | 0.01 | N/A | 2 | N/A | N/A | 151.1 |
| 11 | 320 | 0.00 | 0.00 | 0.00 | N/A | 2 | N/A | N/A | * |

| Station | Depth (m) | AMX Rate (nM $N_2$ $d^{-1}$) | DN Rate (nM $N_2$ $d^{-1}$) | $NO_2^-$ (µM) | $NH_4^+$ (nM) | Added $^{15}NO_2^-$ (µM) | Added $^{15}NH_4^+$ (nM) | $NH_4^+$ Enrichment | $NO_2^-$ Enrichment |
|---|---|---|---|---|---|---|---|---|---|
| 12 | 103 | 2.64 | 1.26 | 0.10 | N/A | 2 | N/A | N/A | 20.6 |
| 12 | 120 | 2.64 | 0.00 | 1.51 | N/A | 2 | N/A | N/A | 2.3 |
| 12 | 150 | 8.72 | 1.91 | 1.18 | N/A | 2 | N/A | N/A | 2.7 |
| 12 | 610 | 0.99 | 1.42 | 0.01 | N/A | 2 | N/A | N/A | 399.9 |
| 14 | 125 | 1.77 | 0.00 | 1.20 | N/A | 2 | N/A | N/A | 2.7 |
| 14 | 323 | 0.00 | 0.34 | 0.00 | N/A | 2 | N/A | N/A | * |
| 15 | 135 | 3.11 | 1.39 | 0.07 | N/A | 2 | N/A | N/A | 31.7 |
| 15 | 160 | 1.39 | 0.00 | 0.67 | N/A | 2 | N/A | N/A | 4.0 |
| 18 | 130 | 2.01 | 0.67 | 0.13 | N/A | 2 | N/A | N/A | 16.6 |
| 18 | 160 | 0.70 | 0.00 | 0.00 | N/A | 2 | N/A | N/A | * |
| 18 | 200 | 0.00 | 0.00 | 0.00 | N/A | 2 | N/A | N/A | * |

**Supplementary Table S7:** $NO_2^-$ and $NH_4^+$ enrichments due to tracer additions in the SR1805 and FK180624 anammox and denitrification rate samples. The columns labeled $NO_2^-$ (µM) and $NH_4^+$ (nM) refer to the ambient concentrations. $NH_4^+$ concentrations, additions, and enrichments are not reported for FK180624 samples because only $^{15}NO_2^-$ additions were performed. Asterisks indicate samples where the ambient $NO_2^-$ was zero and the enrichment calculation could not be carried out.

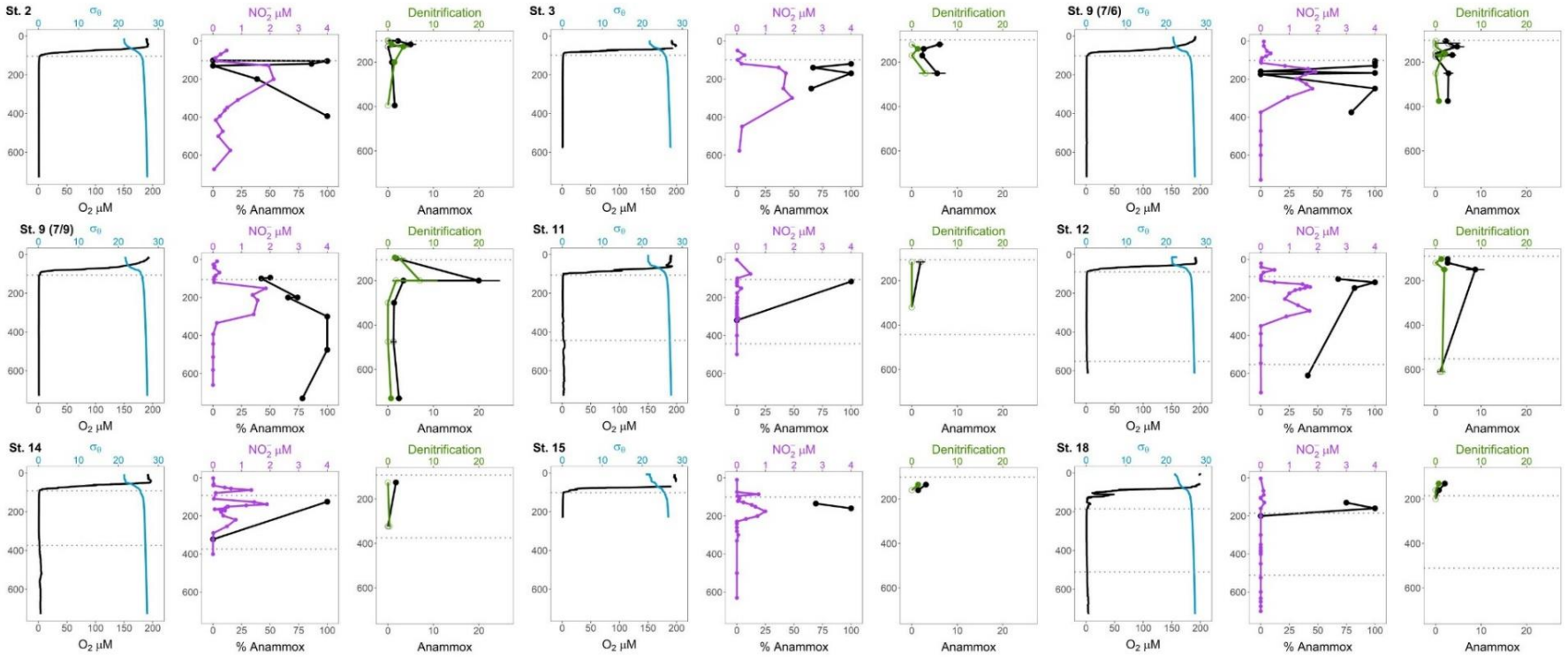


**Figure S1:** Depth profiles of biogeochemical parameters and N loss rate measurements from cruise FK180624. Measurements were conducted at eight stations along a gradient from waters (St. 2 and 3) similar to OMZ station PS2 (SR1805 cruise) to stations near the border of the OMZ region (St. 15 and 18) (Fig. 1). Station 9 was sampled multiple times, once on 7/6/2018 and once on 7/9/2018. For each station, $O_2$ (µM) (black) and $\sigma_\theta$ (kg $m^{-3}$) (cyan) are shown in the first panel, $NO_2^-$ (µM) (purple) and % anammox values (black) are shown in the second panel, and anammox (black) and denitrification rates (green) (nM $N_2$ $d^{-1}$) are shown in the third panel. Grey dotted lines indicate the upper and lower boundaries of the ODZ region at the time of sampling. The bottom boundary was below the edge of the plot in stations 2, 3, and 9 while the CTD did not sample deeply enough to measure this feature for station 15. In the N loss plots, filled circles indicate rates significantly different from zero, while open circles are insignificant rates. Error bars indicate the standard error of the regression.

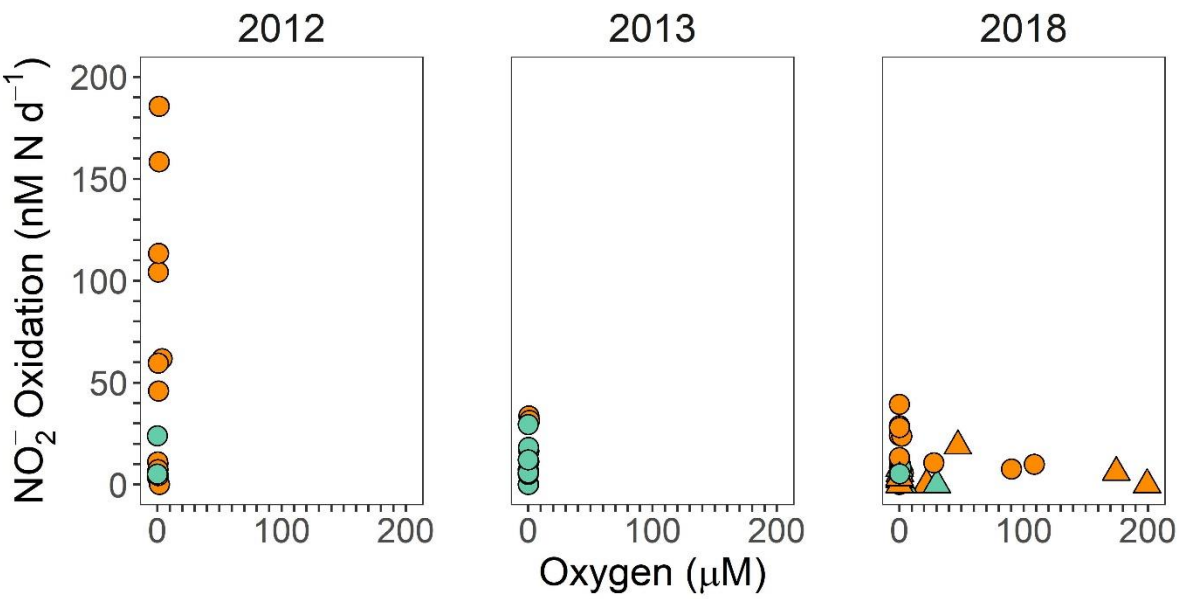


**Figure S2:** $NO_2^-$ oxidation rates (nM N $d^{-1}$) from the TN278, and NBP1305, and SR1805 cruises vs. $O_2$ concentration (μM) from the shipboard CTD sensors. $O_2$ concentrations were normalized across cruises. Rates that are significantly different from zero as assessed via a student T-test (p value < 0.05) are displayed as filled circles, while insignificant rates are displayed as triangles. Rates measured in shallow boundary waters are colored orange while rates from the ODZ core and below are colored teal. 2012 and 2013 data are republished (Babbin et al., 2020).

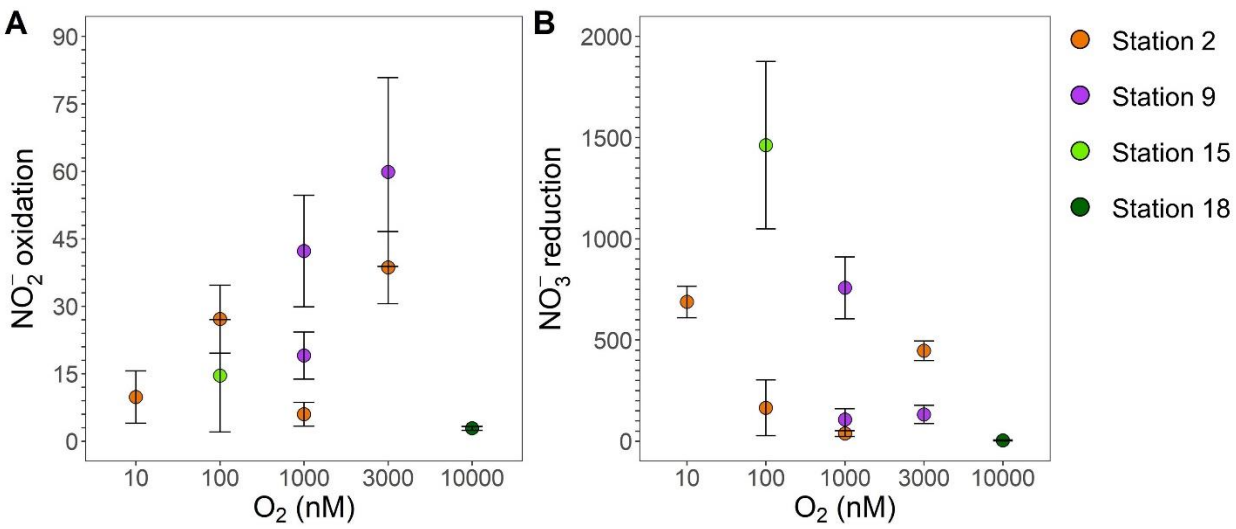


**Figure S3:** $O_2$ manipulation experiments from the FK180624 cruise in summer 2018. $NO_2^-$ oxidation **(A)** and $NO_3^-$ reduction **(B)** (nM N $d^{-1}$) measured across an $O_2$ gradient from 10 to 10000 nM. Station 2 (dark orange) is closest to shore and represents a similar region to station PS2 from cruise SR1805 in spring 2018. Station 9 (purple) is an intermediate environment between station 2 and stations 15 (light green) and 18 (dark green) which are farther offshore and represent the boundaries of the OMZ region (Fig. 1). Error bars represent the standard error of the regression.

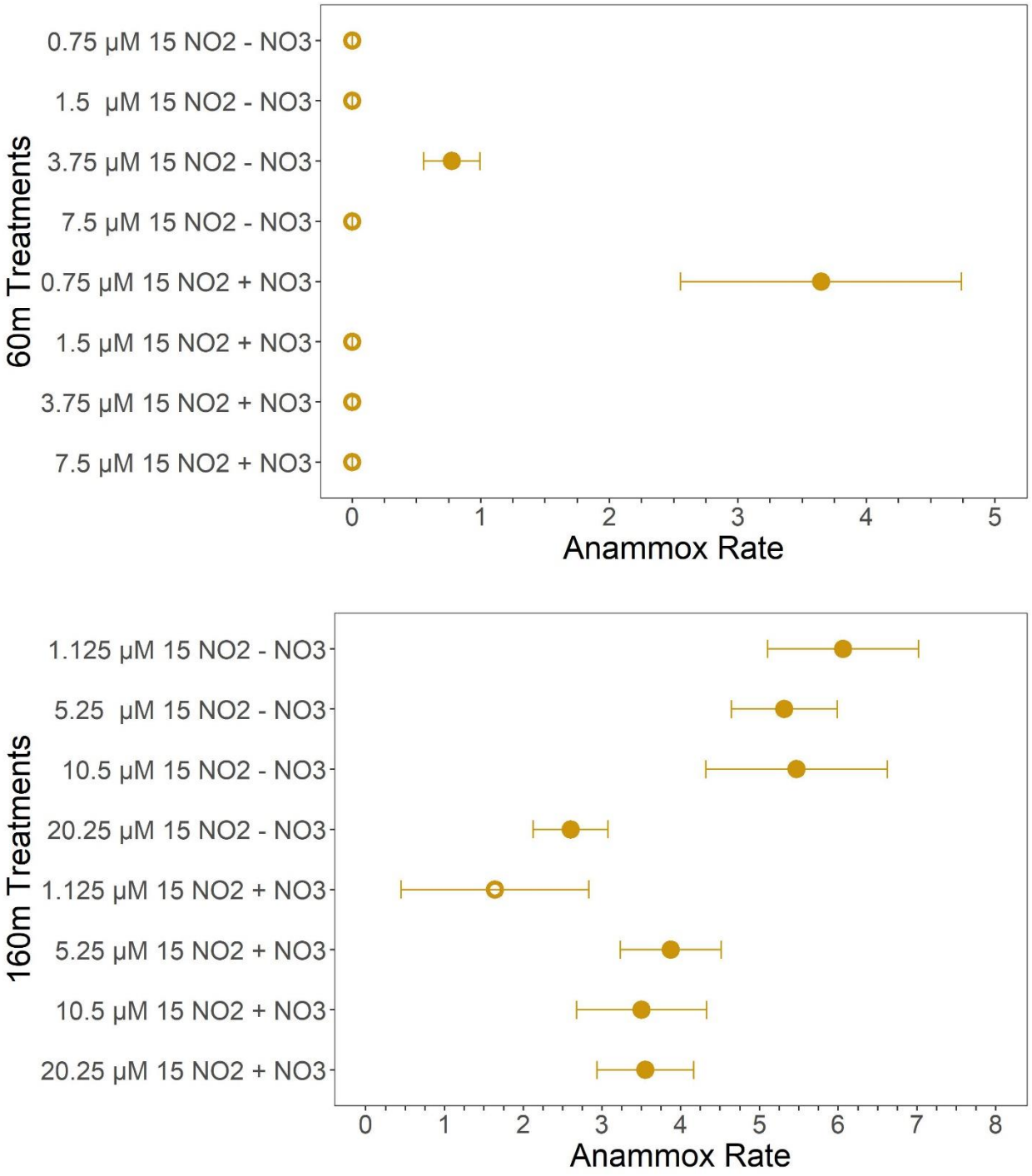


**Figure S4:** Anammox rates (nM $d^{-1}$) used to calculate the unexplained $NO_2^-$ oxidation rate in Fig. 5. Filled circles indicate significant rates while open circles indicate rates that are not significantly different from zero. Error bars are the standard error of the regression.

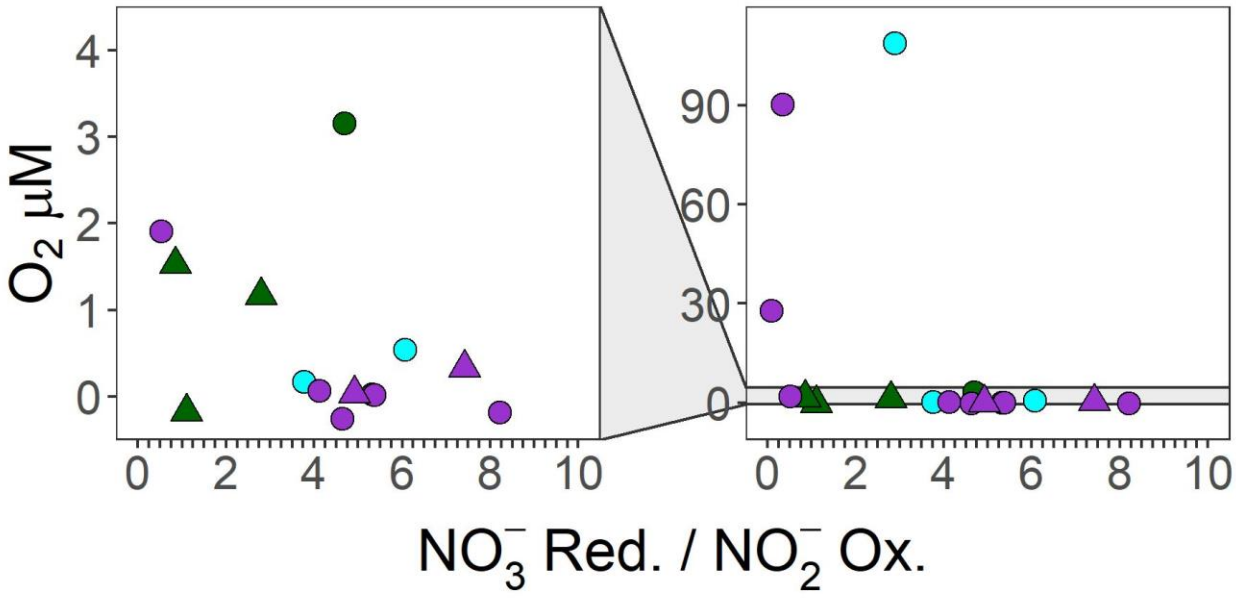


**Figure S5:** Oxygen does not differentially regulate $NO_3^-$ reduction and $NO_2^-$ oxidation. $O_2$ (µM) plotted against the ratio between the $NO_3^-$ reduction rate and $NO_2^-$ oxidation rate for all SR1805 depths with significant $NO_2^-$ oxidation rates. Triangles indicate samples from the ODZ core or below ($\sigma_\theta > 26.4$) and circles depict samples from shallow boundary waters ($\sigma_\theta < 26.4$). Colors indicate station: purple (PS3), green (PS2), cyan (PS1).

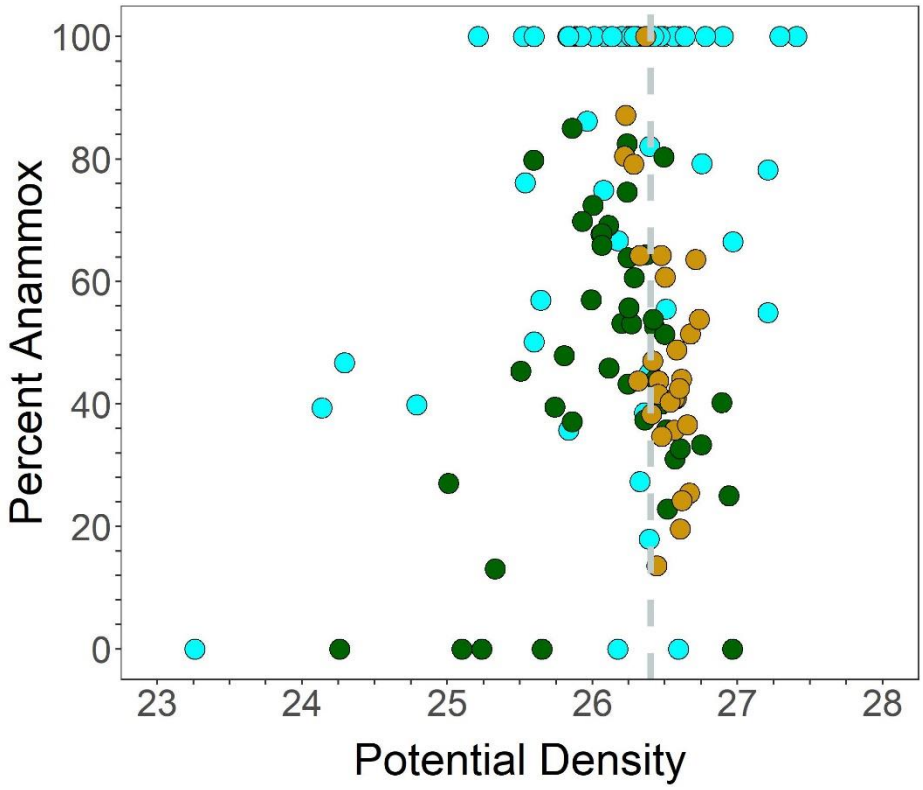


**Figure S6:** Percent anammox plotted against potential density for all cruises. Data from TN278 (ETNP 2012) is shown in green, NBP1305 (ETSP 2013) is shown in gold, and both 2018 cruises (SR1805 and FK180624) in cyan. The grey dashed line differentiates shallow boundary waters ($\sigma_\theta < 26.4$) and waters from the ODZ core and below ($\sigma_\theta > 26.4$).

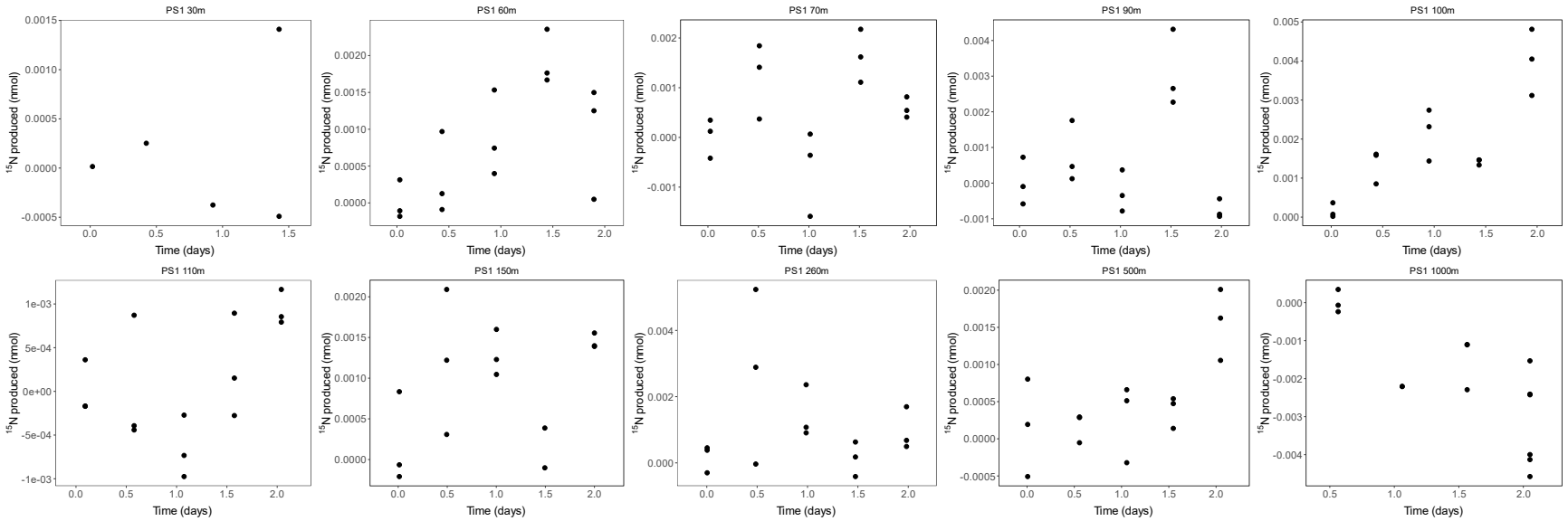


**Figure S7:** Time-courses from SR1805 $NO_2^-$ oxidation depth profile experiments. All depths from station PS1 are shown. Top row, from left to right: 30, 60, 70, 90, 100 m, bottom row from left to right: 110, 150, 260, 500, 1000m. The y-axis depicts $^{15}N$ produced in nmol N while the x axis shows time in days. Complete time-courses are shown. For each depth, the best regression from $t_0 - t_2$, $t_0 - t_3$, or $t_0 - t_4$, was used to calculate the final rate plotted in Fig. 2.

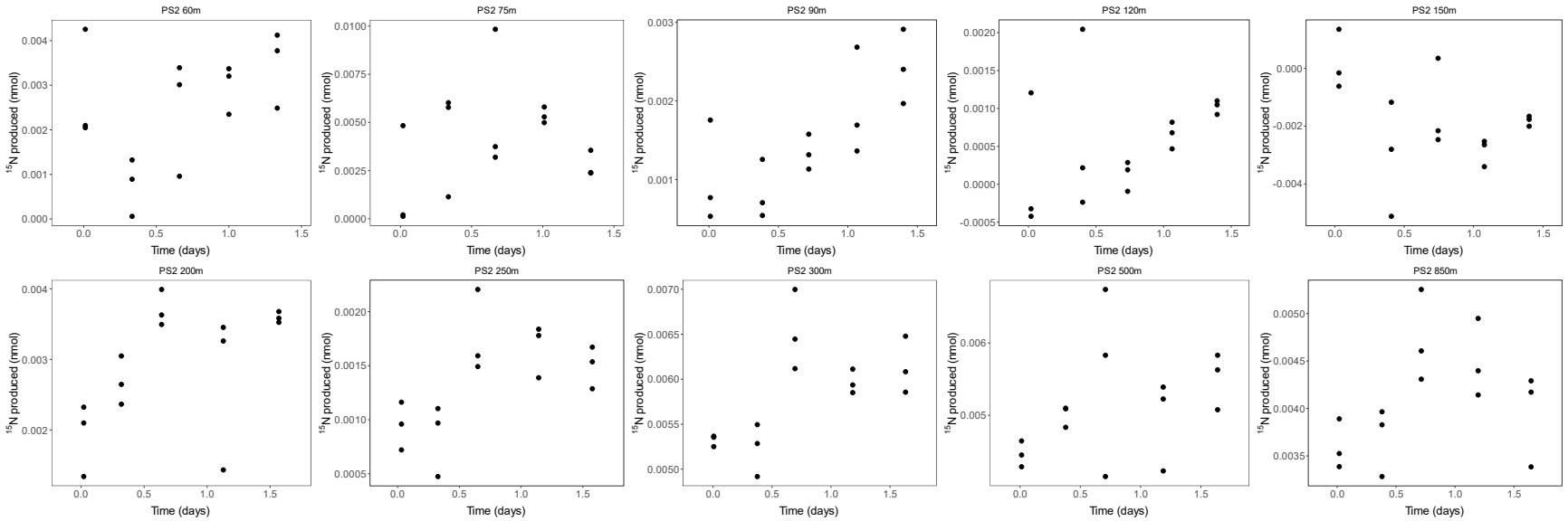


**Figure S8:** Time-courses from SR1805 $NO_2^-$ oxidation depth profile experiments. All depths from station PS2 are shown. Top row from left to right: 60, 75, 90, 120, 150 m, bottom row from left to right: 200, 250, 300, 500, 850m. The y-axis depicts $^{15}N$ produced in nmol N while the x axis shows time in days. Complete time-courses are shown. For each depth, the best regression from $t_0 - t_2$, $t_0 - t_3$, or $t_0 - t_4$, was used to calculate the final rate plotted in Fig. 2.

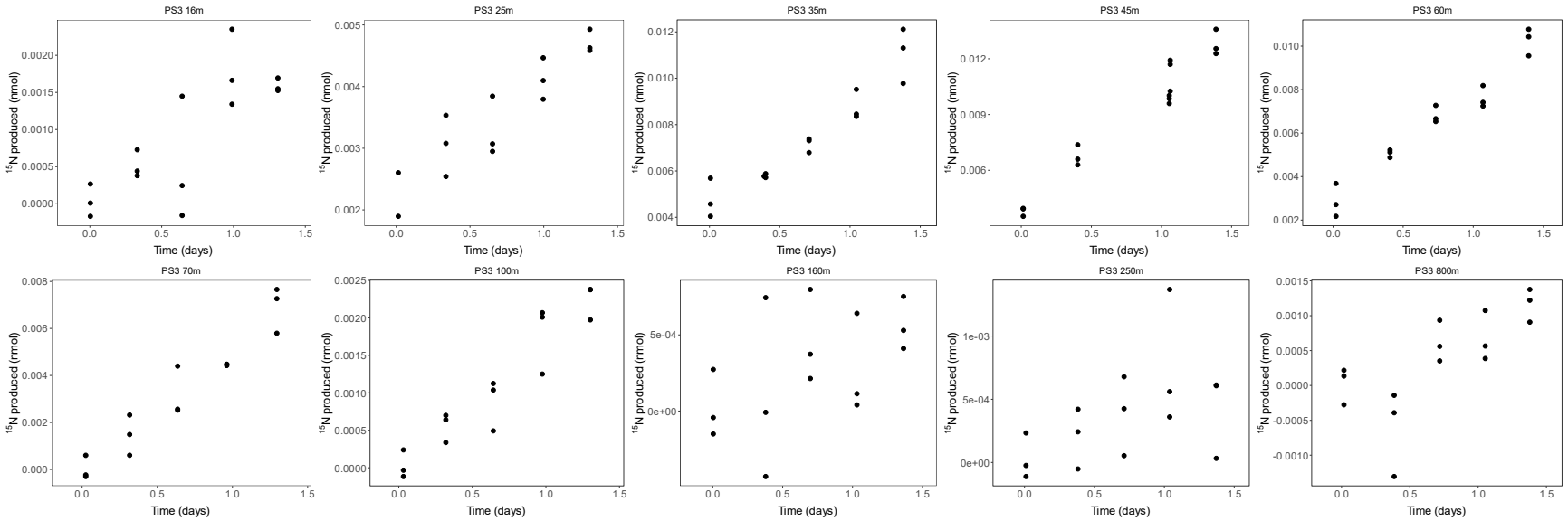


**Figure S9:** Time-courses from SR1805 $NO_2^-$ oxidation depth profile experiments. All depths from station PS3 are shown. Top row from left to right: 16, 25, 35, 45, 60, bottom row from left to right: 70, 100, 160, 250, 800m. The y-axis depicts $^{15}N$ produced in nmol N while the x axis shows time in days. Complete time-courses are shown. For each depth, the best regression from $t_0 - t_2$, $t_0 - t_3$, or $t_0 - t_4$, was used to calculate the final rate plotted in Fig. 2.